



Hygroscopic movements in Geraniaceae: the structural variations that are responsible for coiling or bending

Yael Abraham and Rivka Elbaum

The Smith Institute of Plant Sciences and Genetics in Agriculture, The Hebrew University of Jerusalem, Rehovot, 76100, Israel

Author for correspondence: Rivka Elbaum Tel: +972 8 9489335

Email: rivka.elbaum@mail.huji.ac.il

Received: 10 January 2013 Accepted: 4 March 2013

New Phytologist (2013) **199:** 584–594 **doi**: 10.1111/nph.12254

Key words: cell wall structure, coiling, Geraniaceae, hygroscopic movement, polarized light microscopy, Polscope, smallangle X-ray scattering (SAXS), seed dispersal.

Summary

- The family Geraniaceae is characterized by a beak-like fruit, consisting of five seeds appended by a tapering awn. The awns exhibit coiling or bending hygroscopic movement as part of the seed dispersal strategy. Here we explain the variation in the hygroscopic reaction based on structural principles.
- We examined five representative species from three genera: *Erodium*, *Geranium*, and *Pelargonium*. Using X-ray diffraction, and electron and polarized light microscopy, we measured the cellulose microfibril angles in relation to the cell and cellulose helix axes. The behavior of separated single cells during dehydration was also examined.
- A bi-layered structure characterizes all the representative genera studied, with a hygroscopically contracting inner layer, and a stiff outer layer. We found that the cellulose arrangement in the inner layer is responsible for the type of awn deformation (coiling or bending). In three of the five awns examined, we identified an additional coiling outer sublayer, which adds coiling deformation to the awn.
- We divide the movements into three types: bending, coiling, and coiled-bending. All movement types are found in the *Geranium* genus. These characteristics are of importance for understanding the evolution of seed dispersal mechanisms in the Geraniaceae family.

Introduction

Many plants utilize hygroscopic movement as part of their seed dispersal strategy by employing specialized tissues sensitive to humidity. These dead hygroscopic tissues consist mainly of cell walls made up of stiff crystalline cellulose microfibrils, organized usually in a helix, and embedded in an amorphous matrix of polysaccharides, aromatic compounds and structural proteins. It was first suggested by Zimmerman (Jost, 1907) that passive hygroscopic movement in dead plant tissues is controlled by the orientation of cellulose microfibrils in the cell wall: As the cell wall matrix absorbs water, it expands in a direction that is perpendicular to the stiff microfibrils and deforms the cell. The extent of the cell deformation is determined by the angle between the microfibrils and the cell's long axis, the microfibril angle (MFA) (Lacey et al., 1983; Witztum & Schulgasser, 1995; Dawson et al., 1997; Elbaum et al., 2007; Fratzl et al., 2008; Reyssat & Mahadevan, 2009; Pufal et al., 2010).

One such group of plants utilizing hygroscopic movement is the Geraniaceae family, which consists of five genera: *Geranium*, *Monsonia*, *Pelargonium*, *California* and *Erodium* (Aldasoro *et al.*, 2002; Albers & Vander Walt, 2007). Fig. 1 shows *Erodium gruinum* (L.) L'Hér. as a representative member of the family. One of the main characteristics of this family is a beak-shaped fruit that is made up of five mericarps arranged around an inner central column. The mericaps consist of a capsule encasing the

seed at the base of the fruit, and a long tapering tail (the awn) forming the 'beak' (Fig. 1c). The awns are connected to the central column through dehiscence tissue designed to sustain the awns during growth and to facilitate the timely release of the dispersal units. As the fruit ripens, the awns start to dry and distort (Fig. 1b vs c), resulting in tension accumulating within the structure, until the dehiscence tissue snaps. In most species, the awns coil as they dry, while *Geranium* also includes species with bending awns (Fig. 2; *E. gruinum* movie (http://www.youtube.com/watch?v=Hb2toQRVmCg) (Abraham *et al.*, 2012); Supporting Information Movies S1–S4).

The awn's shape reflects the dispersal mode

The awns display a variety of morphologies that are adapted to different modes of seed dispersal (Fig. 2). Bending awns (only in *Geranium* species) act as catapults to launch the seeds away from the mother plant, with or without the capsule (Yeo, 1984; Herrera, 1991). In species with coiling awns, the seed remains sealed in the capsule and the entire mericarp acts as an independent dispersal unit. When the awn is relatively thin and soft (as in *Pelargonium* and some *Erodium* species), the dispersal unit will remain attached to the top of the central column as it coils. This coiling aligns the long feathery hairs on the awn in a spiral, to form a parachute (pappus-like) that enables it to be dispersed by wind. Both catapult and flight strategies involve a single use of the

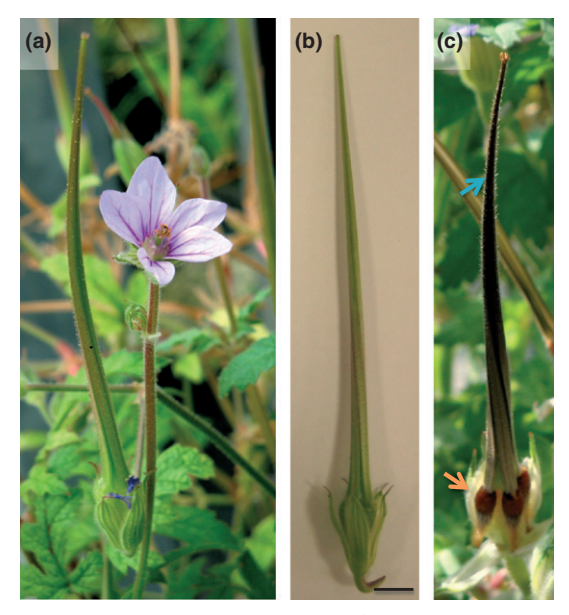


Fig. 1 *Erodium gruinum* as a representative of the Geraniaceae plant family. (a) Flower and beak-shaped fruit. (b) The 'beak' of the fruit consists of five awns attached to the seed capsule at the base of the fruit (bar, 0.5 cm). (c) As the fruit ripens, the awns dehydrate and induce a twisting deformation of the fruit 'beak'. The blue arrow points to the awns forming a beak, while the orange arrow points to the seed capsules.

hygroscopic mechanism. Other species have thicker and stiffer awns that accumulate far more tension as they dry. The snapping of the dehiscence tissue results in the ejection of the dispersal unit away from the mother plant, in some cases to a distance of up to 3 m (Stamp, 1989a,b; Evangelista *et al.*, 2011). Once the dispersal unit reaches the ground, the stiff coiled awn responds to the diurnal humidity cycle and propels the unit across the ground until it becomes lodged in a crevice. At this point, the continued force exerted by the awn pushes the encapsulated seed into the ground to its final germination locus (Stamp, 1984). In these species, the long hairs on the awn point away from the seed, and are much stiffer. Their apparent role is to decrease friction to support movements in the seed direction.

Cellulose microfibril structures leading to hygroscopic bending or coiling

Hygroscopic movement that involves bending is well understood, and was found to be based on a bi-layer construct in which one layer contracts more than the other as it dries, resulting in a bending motion (Fahn & Werker, 1972). In contrast, the structural configuration responsible for the coiling motion in E. gruinum is based on intrinsically coiling cells (Abraham et al., 2012). The cellulose microfibrils in the cell wall of these cells form an unusual tilted helix configuration, in which the helix axis is at an angle to the cell's long axis. We therefore define two angles to describe the direction of the microfibrils: the tilt angle, which is the angle between the cellulose helix axis and the cell's long axis, and the cellulose microfibril angle in relation to the cellulose helix axis (MFAH) (Fig. 3). The normal cellulose helix configuration, in which the tilt angle is zero, is prevalent in cells with a mechanical role (Barnett & Bonham, 2004). As these cells dry, the hygroscopic component of the cell wall (the noncrystalline matrix) contracts isotropically. The nontilted helical cellulose scaffold (Fig. 3a) induces a twist in the drying cell (Gillis & Mark, 1973). When the cellulose microfibril helix is tilted in relation to the cell's long axis (Fig. 3d), a contraction direction that is perpendicular to the cell's long axis is introduced that causes the cell to bend as it is twisting, which results in a coiling cell (Aharoni et al., 2012). Therefore, to induce a coiling movement, only one homogenous layer of these coiling cells is required, in contrast to the bending movement, which requires two different layers. Nevertheless, the E. gruinum awn displays a multilayered structure (Jost, 1907), the role of which is unclear. In addition, all the genera within the Geraniaceae family exhibit coiling awns, suggesting that bending awns evolved from a primitive coiling awn (Yeo, 1984). This raises the question as to the structural variations responsible for the transition from coiling to bending.

Here we examined awns of five representative members of three genera in the Geraniceae family, *Erodium*, *Pelargonium* and *Geranium*, displaying bending and varying types of coiling pitch,

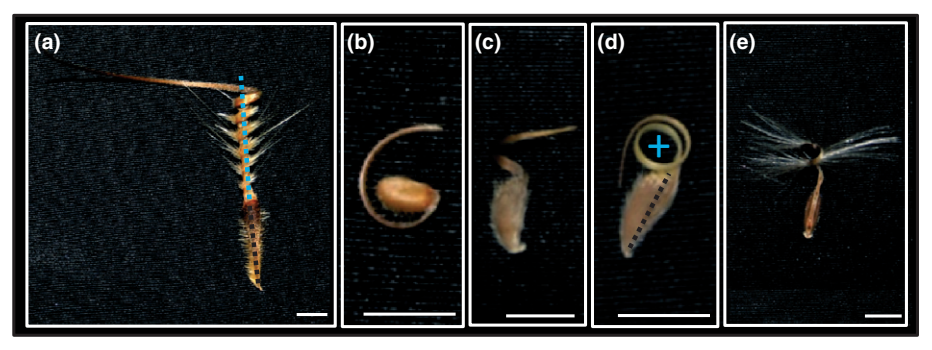


Fig. 2 Geraniaceae dispersal units. (a) The *Erodium gruinum* awn displays a parallel coil in which the coil axis (cyan dotted line) is nearly parallel to the seed capsule axis (black dotted line). (b) *Geranium pusillum* catapult consisting of a bending awn and a pericarp. In contrast to the other examples shown here, this species shoots the seeds away from the mother plant while the awns remain attached to the top of the central column. (c) The *Geranium dolomiticum* dispersal unit exhibits a parallel coil. (d) The *Geranium reflexum* awn displays a perpendicular coil in which the coil axis (represented by a blue +) is nearly perpendicular to the seed capsule axis and the picture plane. (e) The awn of *Pelargonium peltatum* forms a coil which is also parallel to the seed axis. The pronounced hairs form a parachute structure, similar to a pappus (bars, 1 cm).

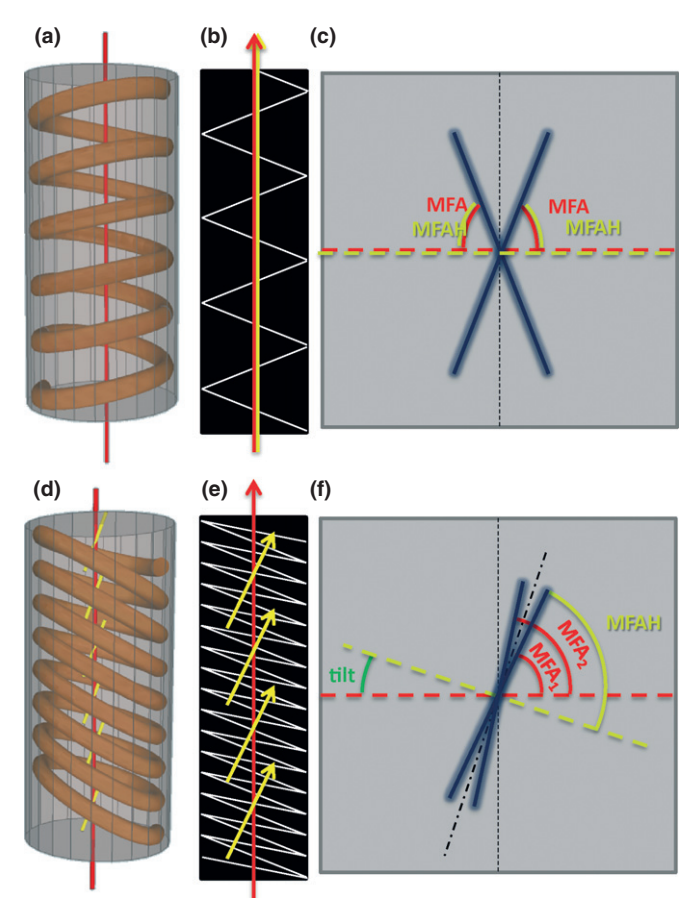


Fig. 3 Cellulose organization within the twisting and coiling cells. (a) Schematic illustration of a cellulose microfibril that is organized in a nontilted helix. The cell's long axis is represented by a red rod. (b) Side projection of the cell wall showing that the cell's long axis (red arrow) lies parallel to the cellulose helix axis (yellow arrow). (c) An illustration of the small angle X-ray scattering (SAXS) pattern that would be produced by a nontilted cellulose helix. The two streaks obtained are perpendicular to the direction of the cellulose microfibrils. The 2D SAXS detector collects a pattern corresponding to the side projection of the cell wall shown in (b). The red dotted line indicates the direction of the cell's long axis, which is parallel to the cellulose helix axis (yellow dotted line). The microfibril angle (MFA) (indicated by a red curved line) is the angle between the streaks and the cell's long axis. As the MFA does not change around the cell wall in a nontilted helix, the MFA obtained for both the streaks is the same. It is also equal to the cellulose microfibril angle in relation to the cellulose helix axis (MFAH), which is the angle between the cellulose microfibrils and the cellulose helix axis (indicated by a yellow curved line). Note that the MFAH value is half the angle between the streaks. (d) Schematic illustration of a cellulose microfibril that is organized in a tilted helix. The cell's long axis is represented by a red rod, and the cellulose helix axis by yellow rods. (e) Side projection of the cell wall showing that the cell's long axis (red arrow) lies at an angle to the cellulose helix axis (yellow arrows). (f) An illustration of the SAXS pattern that would be produced by a tilted cellulose helix. Two different MFAs are obtained in relation to the cell's long axis, represented by MFA₁ and MFA₂, as the MFA changes around the cell wall in a tilted helix configuration. The tilt, which is the angle between the cellulose helix axis and the cell's long axis, is indicated in the illustration by a curved green line.

radius, and alignment in relation to the seed capsule axis (Fig. 2). We report on the structure of the awns and reveal that all of them are essentially made of two layers that differ in their cellulose microfibril angles. Subtle variations in the microfibril helical

arrangement and the appearance of sublayering result in a variety of hygroscopic movements. This structure, rather than the topology of the dried awn, should be correlated to evolutionary trends.

Materials and Methods

Awns from varied sources, as described in the following paragraphs, were kept in ambient conditions. Samples from each species were taken at half the length of the hygroscopically active part of their awn.

Wild mature *Erodium gruinum* (L.) L'Hér. dispersal units were collected in the hills of Nes-Tziona, Israel, on 1 May 2009 and kept in ambient conditions. *Erodium gruinum* was germinated according to the procedure described previously (Young *et al.*, 1974), and dispersal units were continuously collected from the mature plants.

Domesticated mature *Pelargonium peltatum* (L.) L'Hér. dispersal units were collected from a private garden in Rehovot, Israel.

Wild mature *Geranium pusillum* L. dispersal units were collected near Jagotin, Kiev Province, Ukraine, courtesy of Stanislav N. Gorb.

Wild mature *Geranium dolomiticum Rothm.* and *Geranium reflexum L.* dispersal units were obtained from the herbaria of Real Jardín Botánico, Madrid, Spain, courtesy of Carlos Aedo.

Preparation of cross-sections for optical microscopy

The various awns were embedded in polyethylene glycol (PEG) 2000 MW as described elsewhere (Rüggeberg $\it et al.$, 2008). Cross-sections (10 μm thick) from the coiling or bending region were cut on a rotary microtome (Leica RM2255; Leica Biosystems GmbH, Nussloch, Germany), and then placed in water to remove the PEG. The washed cross-sections were placed on a glass slide with a drop of water, and sealed with a cover-slip to prevent evaporation of water during the measurement.

LC-PolScope retardance imaging

The samples' birefringence was investigated using an LC-PolScope image processing system (CRi Inc., Woburn, MA, USA) mounted on a microscope (Nikon Eclipse 80i, Tokyo, Japan) equipped with Plan Fluor X20/0.5 OFN25 DIC N2, Plan Fluor X40/0.75 OFN25 DIC M/N2, and Fluor X60/100w DIC H/N2 ∞ /0 WD 2.0 objectives. The system includes a computer-controlled universal compensator made of two liquid crystal variable retarders. Retardance images were taken by a cooled CCD camera at high optical resolution. Retardance values were extracted manually, using Abrio software tools (CRi Inc.), from at least five cells for each sample.

Scanning electron microscopy (SEM)

Samples from the coiling or bending region of the mature awns were broken by hand. The samples were prepared by critical point drying, mounted on aluminum stubs, and sputter-coated with gold-palladium. Samples were examined in the environmental scanning electron microscope XL 30 ESEM FEG (FEI, Eindhoven,

Netherlands) 10–12 kV, using high vacuum mode, at 9.0–9.5 mm working distance.

Small-angle X-ray scattering (SAXS)

The inner and outer faces of the coiling region of the *E. gruinum* awn were separated in wet awns, using a razor blade. *Pelargonium* peltatum awns were separated after maceration in a solution of 30% H_2O_2 , glacial acetic acid and distilled water (1:5:4) for 1 d at 60° C, based on the method of Brisson, Gardner, and Peterson (Yeung, 1998). The *G. dolomiticum* and *G. reflexum* awns were measured complete, while the awns of *G. pusillum* were provided to us separated. Wet samples were inserted into 1.5-mm quartz capillaries, to which $10 \,\mu l$ of distilled water was added to maintain their wet state. The capillaries were flame-sealed and mounted vertically, in a perpendicular orientation to the X-ray beam. Experiments were carried out at room temperature. Each sample was checked before and after the experiment to verify that no fluid was lost during the time of exposure, c. 1 h.

Scattering experiments were performed using CuKa radiation $(\lambda = 0.154 \text{ nm})$ from a Rigaku-MicroMax 007 HF X-ray generator (Rigaku, The Woodlands, TX, USA) operated at a power rating up to 1.2 kW. The beam size at the sample position was $0.7 \times$ 0.7 mm², as defined by a set of two scatterless slits (Li *et al.*, 2008). The scattered beam went through a flight path filled with helium (He), and reached a Mar345 Image Plate detector (MAR Research, Norderstedt, Hamburg, Germany). The sample distance to the detector was 1841.3 mm, calibrated using silver behenate. Background correction was verified by measuring the scattering of a capillary filled with distilled water and correcting for sample absorption. Integration of the scattering density was performed using FIT2D software (Hammersley et al., 1996). Scattered intensity was plotted as a function of the scattering vector $q = (4\pi/\lambda)$ $\sin\theta$, where λ is the X-ray wavelength and θ is half the angle between the incident and scattered wave vectors (Nadler et al., 2011).

Results

In the first part of this section, we present the general layered structure of the Geraniaceae awn. We then examine what

structural variations are found, and how they affect the awn topology. The last part of the section presents the structure of the *P. peltatum* awns, a member of the Geraniaceae family that is evolutionarily remote from the other species studied.

In order to determine the cellulose organization on a microscopic scale, our strategy in this work was to measure the MFAH range and helical tilt in each awn, using SAXS, and then to correlate the values to the microscopic structure as revealed by polarized light and electron microscopy. When measuring the orientation of cellulose with SAXS, we report the microfibril angles in relation to the cellulose helix axis (MFAH) and its tilt, as illustrated in Fig. 3, while when estimating the angles microscopically, we report the conventional angle relating to the cell's long axis (MFA). In addition, we record the movement of drying single cells isolated from the awns to support our models. The MFAH and tilt angles are summarized in Table 1.

Coiling in *Erodium gruinum* – the basic layered structure of the awn

The coiling *E. gruinum* awn (Fig. 2a) exhibits a cross-section with two main layers (Jost, 1907). We define the layer facing into the coil as the 'inner layer', and the one facing away from the coil as the 'outer layer'. The inner layer is responsible for the coiling of the awn, as the cellulose microfibrils within its cell walls are organized in a tilted helix, inducing coiling in its cells (Abraham *et al.*, 2012).

The SAXS pattern obtained for the isolated outer layer displays two superimposed signals (Fig. 4a): an intense equatorial streak showing an MFAH of c. 10°, and a less intense, fan-like signal tilted by c. 3° off the equator, showing an MFAH of c. 30° (Table 1; see Fig. 3 for angle definitions). Polarized light and SEM revealed that the outer layer indeed consists of two sublayers (Fig. 5). The median sublayer (MidSL) shows low retardance values, seemingly uniform around the cell wall (Fig. 5g), and a brittle and relatively smooth break surface (Fig. 5c). Both these characteristics indicate a cellulose microfibril alignment that is almost parallel to the cell wall axis, and correlated to the SAXS signal for an MFAH of 10°. The outermost sublayer (OutSL) shows a rougher fracture surface (Fig 5b) and higher retardance

Table 1 Values of the tilt angle and the cellulose microfibril angle in relation to the cellulose helix axis (MFAH) of cellulose microfibrils from the five Geraniaceae species (see Fig. 3 for angle definitions), measured by small-angle X-ray scattering (SAXS)

	Erodium gruinum		Geranium pusillum		Geranium dolomiticum		Geranium reflexum		Pelagonium Peltatum	
	Tilt (°)	MFAH (°)	Tilt (°)	MFAH (°)	Tilt (°)	MFAH (°)	Tilt (°)	MFAH (°)	Tilt (°)	MFAH (°)
OutSL	3	30	><	><	><	><	3	25	5	40
MidSL Inner layer	<3 20	10 80 (per) 67 (cen)	0	18 73 (per) 13–35 (mid) 7 (cen)	<3 <3	11 75	0	7 75 (per) 19 (cen)	<3 19	16 70

Based on the retardance images, we assigned the values to the three layers forming the awns: the inner layer, and the outer layer which is divided into two sublayers. Additionally, we identified cell wall laminas within individual cells in the inner layers: the peripheral (per), midway (mid), and central (cen) laminas.

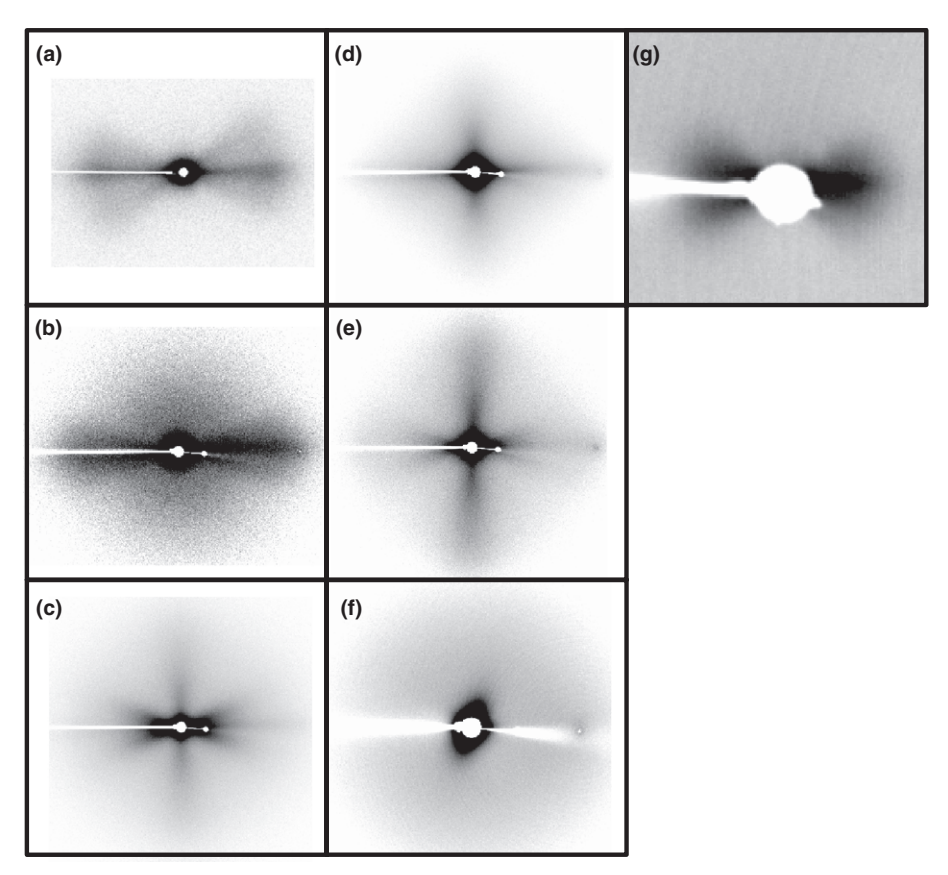


Fig. 4 Small angle X-ray scattering (SAXS) patterns for the different awns. The awns were found to consist of two layers: the outer and inner layers. We define two sublayers within the outer layer – the outermost sublayer (OutSL), which was found in three species of the five examined, and the median sublayer (MidSL), which was found in all the species. We used microscopy data to assign the SAXS signals to a specific sublayer (see text). (a) The SAXS pattern for the outer layer of the Erodium gruinum awn consists of two signals: an intense streak, representing the MidSL, and a fan-like pattern, representing the OutSL, which shows a tilt of 3°. (b) The SAXS pattern for the outer layer of the Geranium pusillum awn consists of a single, fan-shaped equatorial signal. (c) The SAXS pattern for the inner layer of the Geranium pusillum awn shows three superimposed signals on both the meridian and the equator. (d) The SAXS pattern for the complete awn of Geranium dolomiticum shows signals slightly off the equator and the meridian. (e) The SAXS pattern for the complete awn of Geranium reflexum shows a meridional signal, a single streak on the equator and a fan-like signal slightly off the equator. (f) The SAXS pattern for the separated inner layer of the Pelargonium peltatum awn shows a single streak that is off the meridian. (g) The SAXS pattern for the separated outer layer of the Pelargonium peltatum awn shows a weak fan-like pattern off the equator (the OutSL), and a pronounced equatorial streak (the MidSL).

values, which change around the cell wall (Fig. 5f), indicating a correlation to the SAXS signal for an MFAH of 30°, with a tilt angle of 3°. Mechanically separated cells from the outer layer revealed two movement types: cells that coil very slightly, with a small coil radius and relatively large pitch (Movie S5), and cells that show a more pronounced coil, with a bigger coil radius and smaller pitch (Movie S6). We assign the two cell groups to the two layers we detected microscopically, and conclude that the coiling cells with the larger coil radius are from the OutSL and contain tilted cellulose fibrils (Aharoni *et al.*, 2012). The slight coiling movement of the first cell group indicates a low MFAH, probably attributable to cells belonging to the MidSL. However, the tilt in the MidSL is lower than 3°, and therefore too small to measure by SAXS. For an extended discussion of the effect of tissue stiffness on the tilt detection limits, see Notes S1 and Fig. S1.

The SAXS pattern of the inner layer appears to consist of an intense streak tilted at an angle of 20°, which is diffusing into a wider signal (Abraham *et al.*, 2012). LC-PolScope retardance

images reveal that the inner layer is built of uniform cells. However, in each cell we identified a radial gradient of retardance values (Fig. 5h), indicating a corresponding gradient in the MFAs. Based on the retardance and SAXS data, we calculated the MFAHs along the cell radius from the cell periphery to its center (Abraham & Elbaum, 2013). The peripheral cell wall consists of cellulose helices with an MFAH of *c*. 80°, while in the central cell wall the MFAH is *c*. 66°.

Variations in the structure leading to variations in the hygroscopic movement

Bending in *Geranium pusillum* We found that the *G. pusillum* awn is constructed as a classic bi-layered bending apparatus. Scanning electron and polarized light microscopy images of the awn cross-section reveal a bi-layered structure (Fig. 6). The outer uniform layer shows brittle cell wall break morphology (Fig. 6b) and low retardance values (Fig. 6e), indicating a small MFA.

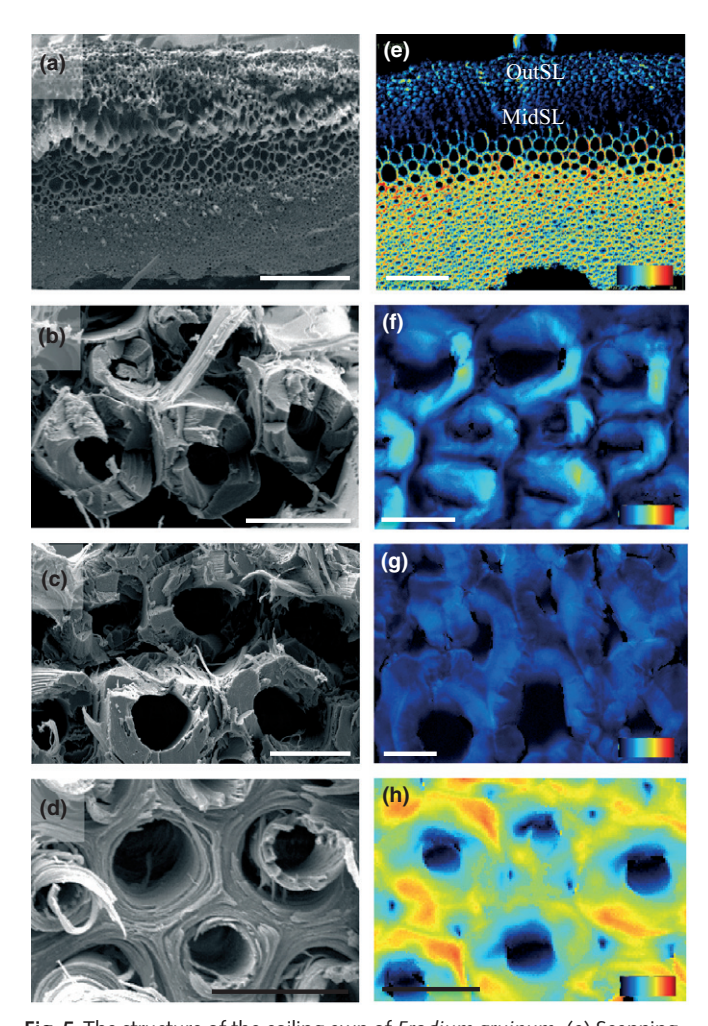


Fig. 5 The structure of the coiling awn of Erodium gruinum. (a) Scanning electron micrographs revealing a layered structure (bar, 200 μ m). A higher magnification reveals three distinct cell wall break morphologies that divide the awn into three regions: two sublayers within the outer layerthe outermost sublayer (OutSL) (b) and the median sublayer (MidSL) (c) and the inner layer (d) (bar, 10 μ m). (e) An LC-PolScope retardance image of a 10- μ m cross-section of the awn reveals the different retardance values supporting variation in the cellulose microfibril angle in relation to the cellulose helix axis (MFAH) between the three layers (bar, 100 µm; retardance range, 27-259 nm). (f) A close-up view of the OutSL shows cell walls with changing retardance as a function of the azimuthal angle. (g) The low retardance values in the outer layer show slight changes around the cell wall that cannot be correlated to the tilting of the cellulose helix due to the layer's high stiffness (see Supporting Information Notes S1 for a discussion of the limits of detection of tilt angles). (h) The inner layer shows relatively high changing retardance values as a function of azimuthal angle and radial distance (bar, 10 μm; retardance range, 0-273 nm).

Mechanically separated single cells from this layer twist slightly as they dry (Movie S7), which suggests that the cellulose microfibrils are organized in a nontilted helix (Aharoni *et al.*, 2012).

The mechanically separated layers of the awn gave two distinct SAXS patterns. The outer layer produced an equatorial nontilted SAXS streak (Fig. 4b), corresponding to a relatively small MFAH of *c*. 18° (Table 1). The low MFAH angle in this layer is reminiscent of the low MFAH found in the midSL cell walls in the *E. gruinum* awn. In contrast, the inner layer produced a more

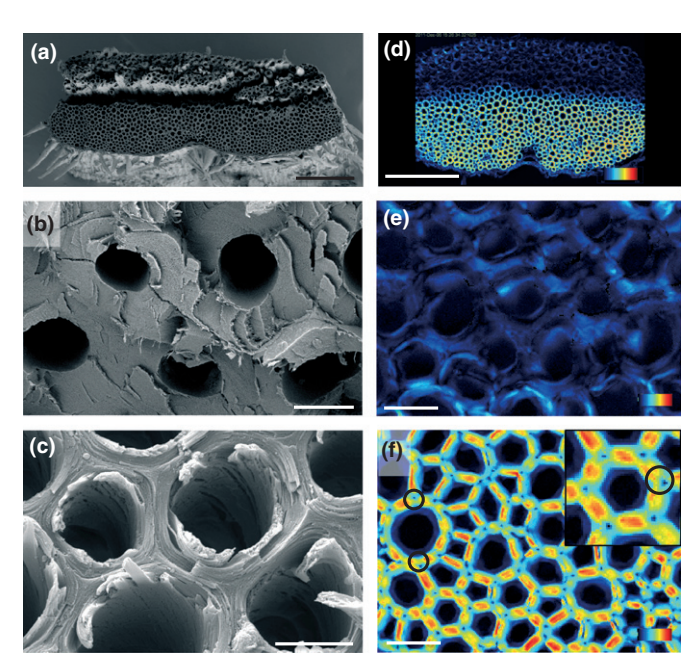


Fig. 6 The layered structure of the *Geranium pusillum* awn. (a) Scanning electron micrographs of a cross-section of the awn revealing its bi-layered structure (bar, 100 μm). (b, c) Close-up views of the outer (b) and inner (c) layers (bar, 5 μm). (d) An LC-PolScope retardance image of a 10-μm cross-section showing the variation in retardance values between the inner and outer layers (bar, 100 μm; retardance range, 0–273 nm). (e) A close-up view of the outer layer reveals changes in the low retardance values around the cell wall, which are inconsistent with a zero tilt (Notes S1) (bar, $10 \mu m$; retardance range, 0–147 nm). (f) The inner layer has high retardance values in the cell wall body while in the wall corners (marked with circles) the retardance is lower. Inset: close-up view of one of the cells (bar, $10 \mu m$; retardance range, 0–273 nm).

complex SAXS pattern of three superimposed signals (Fig. 4c): a meridional line corresponding to a mean MFAH of c. 73°, a crossed two-streak pattern around the equatorial corresponding to an angle range of 13-35°, and an equatorial thin streak indicating a cellulose microfibril population at an MFAH of c. 7°. All the signals are nontilted. Microscopic images showed low retardance signals at the cell wall corners - the curved part of the cell wall facing the meeting points between three neighboring cells (angular span of a corner c. $10-30^{\circ}$). We attribute these low retardance values to variations in the cellulose concentration resulting from the cell wall high curvature, rather than microfibril orientation (see Abraham & Elbaum, 2013, for extended discussion). We identified no major variations between cells in this layer (Fig. 6c, f), similarly to the inner layer of the *E. gruinum* awn. Thus, the variation in the MFAH must originate from lamellas in the cell wall. The retardance values along the cell radius were plotted to illustrate this effect (Fig. 7, Table 1). The MFA appears to have changed at different cell wall deposition stages; in the older, peripheral cell wall, the cellulose microfibrils have a large MFA (high retardance), while in the younger, central cell wall, the MFA appears to be much smaller (low retardance). The gradual reduction in the cell wall MFA may allow longitudinal shortening of the cells as they dry with very little twisting (Movie S8). The twisting of the drying separated cells further indicates a nontilted cellulose arrangement. This conclusion is supported by the symmetric cog-wheel

retardance pattern around the cells, which indicates that the MFA around the cell does not change.

Coiling in the *Geranium* genus We identified two types of coiling movements in the *Geranium* genus: a coil with an axis parallel to the long axis of the seed capsule (*G. dolomiticum*; Fig. 2c, Movie S2), or perpendicular to it (*G. reflexum*, Fig. 2d, Movie S3). Here, we present the structural differences leading to these distinct deformations.

The SAXS pattern of the entire awn of G. dolomiticum (Fig. 4d) shows two superimposed signals: an equatorial streak showing an MFAH of c. 11°, and a second meridional signal corresponding to an MFAH of c. 75°. Microscopic images of the awn cross-section reveal a bi-layer structure with uniform layers (Fig. 8). We assign the low MFAH value of 11° to the outer layer, based on low retardance values (Fig. 8d) and rough fracture morphology (Fig. 8b). The inner layer's spool-like fracture morphology (Fig. 8c) and high retardance values (Fig. 8f) correspond to an MFAH value of 75°. In the softer inner layer, we could identify variation in the retardance around the cell wall, which indicates a tilted helix. Mechanically separated groups of cells from both the inner and outer layers were found to produce a coil with a small pitch angle (Movies S9 and S10, respectively). This indicates a cellulose microfibril helix configuration that is tilted at an angle smaller than 3° (Notes S1).

The second type of coiling, displayed by the awn of *G. reflexum*, is perpendicular to the long axis of the seed capsule (Fig. 2d). The SAXS pattern of the entire awn consists of three signals (Fig 4e): a signal on the meridian, corresponding to a relatively large MFAH of *c.* 75°; an equatorial signal, corresponding to an MFAH of 25° tilted at 3°. Microscopic examination of the cross-section revealed a tri-layered structure (Fig. 9). The retardance in the inner layer is high and radially symmetric around the cell wall (Fig. 9h), and the fracture morphology of the cells is spool-like (Fig. 9d). We thus assign the inner layer an MFAH value of 75°. The middle layer, which has low retardance values

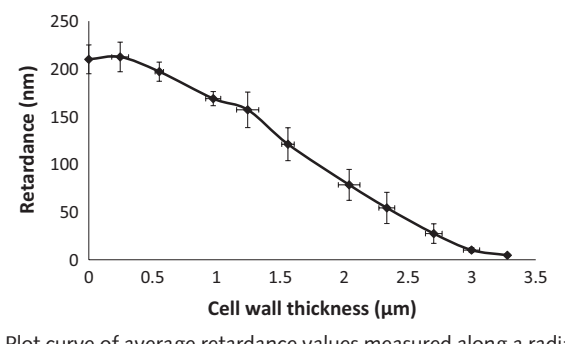


Fig. 7 Plot curve of average retardance values measured along a radial line from the outer layer of the cell wall into the cell. The plot illustrates the reduction in the microfibril angle (MFA) in the $Geranium\ pusillum\ cell$ wall during its development, because the retardance values correspond to the relative MFA values. The retardance values are extracted from the cell wall body (cell wall corners omitted) of five cells. The variations in the cell wall thickness stem from the fact that the cell walls sampled varied in thickness (average thickness $3.3\pm0.2\ \mu m$). The error bars represent standard deviation.

(Fig. 9g) and brittle fracture morphology (Fig. 9c), is similar to the MidSL we defined in the *E. gruinum* awn. We assign to this layer an MFAH value of 7°. The retardance images of the outermost layer, the OutSL, indicate a tilted configuration of the cellulose helix, as they reveal changing retardance values as a function of the azimuthal angle (Fig. 9f). We assign to this layer an MFAH of 25°, tilted at 3°. Mechanically separated cells from the inner layer twist as they dry (Movie S11). This indicates a normal cellulose helix configuration. In contrast, the outer layer consists of two types of cell: twisting cells (Movie S12), which may be related to MidSL, and coiling cells (Movie S13), which indicate a tilted helix configuration, typical of OutSL.

A variation on coiling: *Pelargonium peltatum* The awns of *P. peltatum* are very thin and delicate. Microscopic examination of the cross-section revealed a tri-layered structure (Fig. 10). The SAXS pattern of the inner layer consists of a single streak, tilted at an angle of 19°, corresponding to an MFAH of *c.* 70° (Fig. 4f). The micrographs reveal that the inner layer consists of a single row of large cells of *c.* 80 μm in diameter with changing

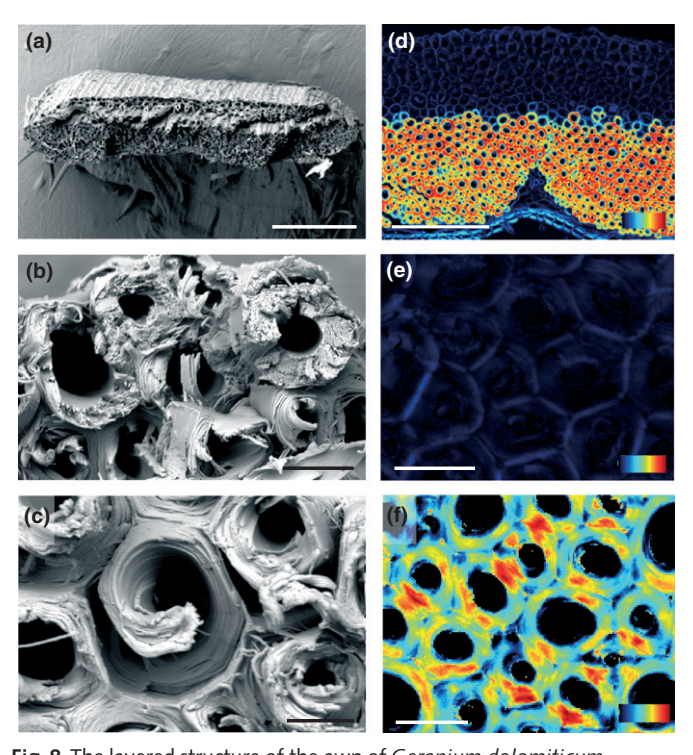


Fig. 8 The layered structure of the awn of *Geranium dolomiticum*. (a) Scanning electron micrographs of a cross-section of the awn revealing its bi-layered structure (bar, 200 μm). (b, c) Close-up views of the outer (b) (bar, 10 μm) and inner (c) (bar, 5 μm) layers show the variation in the fracture characteristics (see text). (d) An LC-PolScope retardance image of a 10-μm cross-section of the awn reveals the different retardance values of the different layers (bar, 100 μm; retardance range, 0–273 nm). (e) The low retardance values in the outer layer show slight changes around the cell wall that cannot be correlated to the tilting of the cellulose helix due to the layer's high stiffness (Notes S1) (bar, 10 μm; retardance range, 0–267 nm). (f) Close-up view of the inner layer shows high retardance values varying azimuthally, similarly to the *Erodium gruinum* inner layer (Fig. 5h). However, the retardance range of 158–273 nm is much smaller than that detected in *Erodium gruinum*, in accordance with a very small tilt in the cellulose microfibril helix (bar, 10 μm).

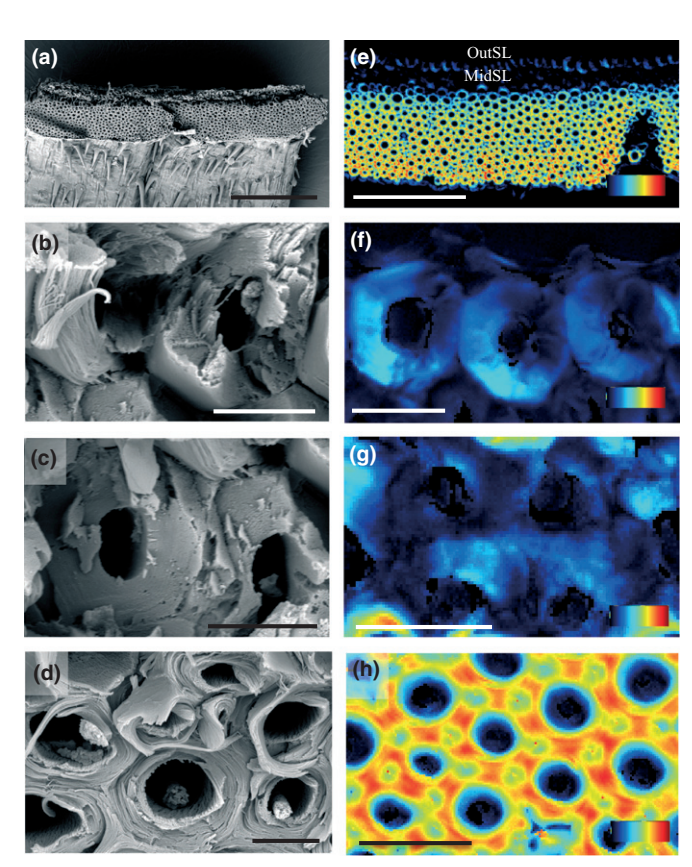


Fig. 9 The layered structure of the Geranium reflexum awn. (a) Scanning electron micrographs of a cross-section revealing a general bi-layered structure with a pronounced inner layer (bar, 200 µm). (b-d) Higher magnifications show two sublayers within the outer layer with different break morphologies, the outermost sublayer (OutSL) (b) and the median sublayer (MidSL) (c), and a uniform inner layer (d) (bars, 5 um), (e) The three layers exhibit different patterns of retardance, as detected by the LC-PolScope system (bar, 100 μm; retardance range, 33–273 nm). (f) Higher magnifications reveal the variation in retardance around the cells' circumference in the outermost sublayer (OutSL), indicating a tilted cellulose helix (bar, 10 µm; retardance range, 0–215 nm). (g) A close-up view of the median sublayer (MidSL) reveals changes in the low retardance values around the cell wall, which are inconsistent with a zero tilt (Notes S1) (bar, 10 μm; retardance range, 0–128 nm). (h) The inner layer has a cog-wheel-shaped high-retardance pattern, with a ring of low retardance in the middle (bar, 10 µm; retardance range, 0-273 nm).

retardance values, supporting the SAXS analysis. The outer layer displays two superimposed SAXS signals: a weak fan-like signal of MFAH 40° tilted at 5°, and an equatorial intense streak at 16° MFAH (Fig. 4g). The retardance images reveal two sublayers forming the outer layer. The OutSL has relatively high retardance values that change around the cell wall (Fig 10e), indicating that the SAXS fan-like signal originates from this layer. The MidSL appears dark blue, consistent with the small MFAH signal detected by the SAXS (Fig. 10f). This bi-layered structure of the outer layer could not be determined based on the SEM image, as the cells appear to have been crushed during the process of fracturing the awn. We were not able to separate single cells from the awns. However, the complete inner layer coils (Movie S14), while groups of cells from the outer layer twist as they dry (Movie S15). Our angle assignments are summarized in Table 1.

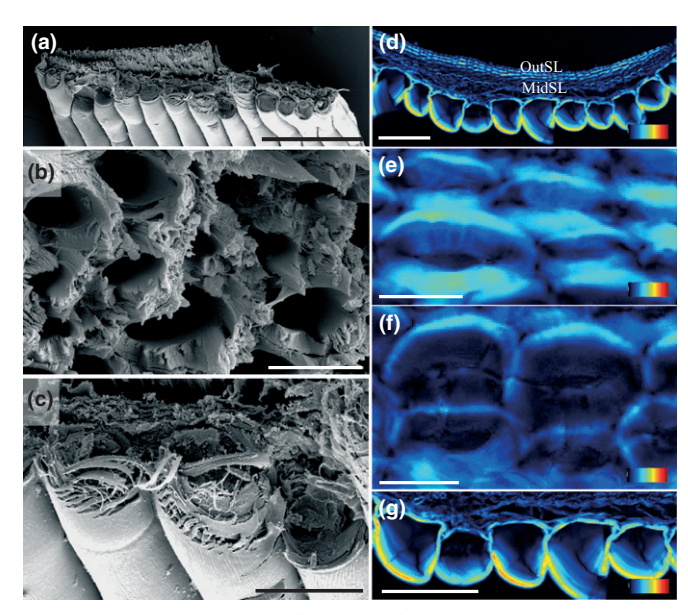


Fig. 10 The layered structure of the awn of *Pelargonium peltatum*. (a) Scanning electron micrographs of a cross-section of the awn revealing a layered structure (bar, 200 µm). (b) Higher magnification of the outer layer reveals a rough break morphology which is indicative of a mid-range microfibril angle (MFA) (bar, 10 μm). (c) An image of the inner layer shows the damage inflicted by the break on the relatively large cells with thin cell walls (bar, 50 μm). (d) An LC-PolScope retardance image of a 10-μm cross-section of the awn reveals three different layers (bar, 100 µm; retardance range, 0-273 nm). (e-g) Close-up views of the different layers of the awn: (e) the outermost sublayer (OutSL) displays a change in the low retardance values as a function of the azimuthal angle (bar, $10 \mu m$; retardance range, 0-273 nm); (f) the median sublayer (MidSL) shows generally very low retardance values, with some variations that are consistent with layering within the cell wall (bar, 10 µm; retardance range, 0-171 nm); (g) the inner layer has changing retardance values as a function of the azimuthal angle (bar, 100 µm; retardance range, 0-273 nm)

Discussion

Data analysis

We present in this work four independent methodologies to assess the properties of the Geraniaceae awns' mechanical tissues, each contributing a specific aspect to the analysis. SAXS allows us to measure directly the average tilt and MFAH angles. However, a tilted SAXS pattern may result either from an inherent tilt of the microfibrils or from a global tilt of the awn sample measured. Therefore, to detect small tilt angles (<3°), other methodologies must be employed. We find the hygroscopic movement of isolated cells to be very sensitive to tilt angles. Combined information from SAXS and cell deformation allows us to distinguish between global and inherent tilt angles. In order to map the cell wall architecture to a specific layer within the awn, we employ polarized light and electron microscopy. Both methods indicate whether the MFA is small or large in the examined layers. In addition, polarized light micrographs allow us to assess whether the microfibril helix is tilted, independently of the SAXS and cell movement (provided that the MFA is larger than 20°; Notes S1 and Fig. S1). Thus, we are able to resolve the awn microstructure

on a subcellular level, and elucidate its effect on the awn hygroscopic deformations.

A generalized structure for the Geraniaceae awns

In general, the awns are bi-layered. Based on our findings, we assign a mechanical role to each layer (Table 2). The inner layer, which experiences the greatest deformation as it dries, exhibits a high MFAH, as expected for an active contracting tissue. This layer determines whether the awn will generally bend or coil; an inner layer built of cells with normal cellulose helices will result in a bending awn, while a layer made of coiling cells (with a tilted cellulose helix) will drive the awn into a coil. The outer layer, with a relatively low MFAH (10-20°) and a helix tilt of 0-2°, stiffens the awn. In catapulting/ejecting dispersal units, high awn stiffness is crucial for tension accumulation during drying. In three species, the outer layer exhibits an additional sublayer (OutSL) consisting of coiling cells, with a slightly higher tilt (2.5-5°) and MFAH (25-40°) (Table 1). The Geranium genus exhibits a variety of seed dispersal mechanisms that employ awns with bending or coiling deformations (Yeo, 1984). Comparing the structure variations within this genus allows us to assign a function to each of the layers we identified.

Geranium pusillum represents the bending awns in this study. The awns are made up of two layers that contract differentially as they dry, similarly to bimetallic thermostats. The same construction was found in other bending hygroscopic systems such as pine (Pinus radiata) cone scales (Dawson et al., 1997), wheat (Triticum turgidum) awns (Elbaum et al., 2007), and Acanthaceae ejaculating fruits (Witztum & Schulgasser, 1995). The awns of G. reflexum are built similarly, in essence; however, they have the additional coiling layer, the OutSL. This arrangement results in a change of the awn deformation from a bend, which creates a two-dimension spiral, to a bend with a 'twist'. This type of deformation is recognized as a three-dimensional spiral, meaning a coil, that is perpendicular to the seed capsule. In contrast, in the bi-layered structure of G. dolomiticum, the active inner layer is built of coiling cells. The resulting shape is a coil with only one or two revolutions and a large relative radius. The awns of E. gruinum and P. peltatum, that have the additional coiling

OutSL, display a tighter coil with more revolutions (six for the E. gruinum awn, and about three for P. peltatum) (Fig. 2; E. gruinum movie (http://www.youtube.com/watch?v=Hb2to-QRVmCg) (Abraham et al., 2012); Movies S2, S4). The separated inner layer from all the coiling awns displays tighter coiling with more revolutions, as compared with the complete awn. We therefore conclude that the MidSL resists the coiling and as a result dampens the deformation. The OutSL tightens the coil back, and when it is missing (in G. dolmiticum) the awn twists less and shows fewer revolutions with a larger radius. In coiling awns, the OutSL works with the inner layer to mitigate the effect of the stiff MidSL, while still giving the awn enough stiffness to function. Our conclusions are summarized in Table 2. Evaluation of additional species with coiling awns along with computational modeling of this effect is required to confirm this hypothesis.

The layered structure of the awn as an evolutionary marker

The beak-shaped fruit was one of the first traits that were used to classify the Geraniaceae family (Aiton, 1789; L'Heritier, 1792; Albers & Vander Walt, 2007; Fiz et al., 2008). The differences in the fruit and other morphological traits, such as awn deformation, leaf and flower shape and the number of nectaries, were used for initial classification within the family, but their high variability made the exact determination of relationships between and within the genera difficult (Fiz et al., 2008). Specifically, the deformation type of the awn is difficult to use in phylogenetic mapping, because in all genera except *Geranium* the awn coils. Subsequently, genetic sequence analysis, combined with other morphological and cytological characters, was used to further strengthen and fine-tune the initial classification (Price & Palmer, 1993; Aldasoro et al., 2002; Fiz et al., 2008; Fiz-Palacios et al., 2010).

We propose that the layered structure of the awn should be considered as another means to classify the groups, by examination of the number of layers, the MFAH and tilt, and the cell size. This approach addresses slight changes in the coiling of the awn that are hard to define otherwise, and may be beneficial for low-level classification within the *Geranium* genus. Based on the traits

 Table 2
 Summary of the layered structure in the five species examined

		Erodium gruinum	Geranium pusillum	Geranium dolomiticum	Geranium reflexum	Pelagonium peltatum
Outer layer	Outer sublayer 10° < MFAH ≪ 90°	Tilted helix; tightening of coil			Tilted helix; tightening of coil	Tilted helix; tightening of coil
	Median sublayer MFAH ~ 10°	Tilted helix; stiffness	Normal helix; stiffness	Tilted helix; stiffness	Normal helix; stiffness	Tilted helix; stiffness
Inner layer	MFAH ~ 90°	Tilted helix; contraction	Normal helix; contraction	Tilted helix; contraction	Normal helix; contraction	Tilted helix; contraction
	Awn deformation	Parallel coil	Bending	Parallel coil	Perpendicular coil	Parallel coil

For each layer, the cellulose helix alignment and the assumed role during dehydration are indicated.

Downloaded from https://nph.onlinelibrary.wiley.com/doi/10.1111/nph.12254 by Cochrane Israel, Wiley Online Library on [23/04/2025]. See the Terms and Conditions (https://onlinelibrary.wiley.com/terms and-conditions) on Wiley Online Library for rules of use; OA articles are governed by the applicable Creative Commons Licensu

proposed, we suggest the definition of four deformations within the family: bending (where the awn has a classical bi-layered structure),

bi-layered coiling (where the awn consists of two layers, with a coiling inner layer), tri-layered coiling (similar to bi-layered coiling, with an additional OutSL), and bended-coiling (similar to bending, with an additional coiling OutSL). Mapping these morphological traits onto a species-level phylogenetic tree may reveal whether similar movement types evolved multiple times independently.

Conclusions

We have shown that all the species studied share a bi-layered structure, in which the inner layer is mainly responsible for the hygroscopic movement, and determines the main mode of deformation that is either a coiling or a bending motion. A stiff outer layer supports the awn mechanically and enables it to keep its shape under minor or major mechanical challenges. An additional sublayer, flanking the outer layer, modulates the extent of the movement by resisting the outer layer's tendency to increase the coil radius. This is based on our observation that once the complete outer layer is removed, the inner layer coil is tighter (Abraham *et al.*, 2012). However, we cannot rule out the possibility that the OutSL prevents the separation of the active and stiff layers as they dry. A mechanical model that assesses the inner strains within the awns may resolve this issue.

The elucidation of awn structure has revealed a way in which awns are adapted to their role in dispersal. For example, the E. gruinum awn is capable of ejecting the dispersal unit away from the mother plant, propelling it across a surface, and burying the seed. Its structure reveals a layered organization in which both the outer and inner layers consist of multiple rows of cell walls, which are relatively thick (c. 7 µm). This gives the awn the stiffness and robustness it requires. In contrast, the P. peltatum awn, which relies on wind dispersal, has an inner layer that consists of only one row of exceptionally big cells with thin cell walls (c. 3 µm). This structure enables the awn to minimize its weight density and still form the coil that organizes the long hairs on the awn in a pappus-like parachute. We have shown that seemingly similar deformations stem from distinctly different structures that can be well defined in terms of the layering of the awn, the tilting of the cellulose helix and the cell size. These characteristics may be used to understand the evolution of seed dispersal mechanisms in the Geraniaceae family.

Acknowledgements

We thank Carmen Tamburu and Uri Raviv (Institute of Chemistry, The Hebrew University of Jerusalem) for the X-ray scattering measurements, and Carlos Aedo (Real Jardín Botánico, Madrid) and Stanislav Gorb (Zoological Institute of the University of Kiel) for the *Geranium* awns and their valuable comments on the manuscript. The electron microscopy studies were conducted at the Irving and Cherna Moskowitz Centre for Nano and Bio-Nano

Imaging at the Weizmann Institute of Science. This research was supported by the Israel Science Foundation through grant 598/10.

References

- Abraham Y, Elbaum R. 2013. Quantification of microfibril angle in secondary cell walls at sub-cellular resolution by means of polarized light microscopy. New Phytologist 97: 1012–1019.
- Abraham Y, Tamburu C, Klein E, Dunlop JWC, Fratzl P, Raviv U, Elbaum R. 2012. Tilted cellulose arrangement as a novel mechanism for hygroscopic coiling in the Stork's Bill awn. *Journal of Royal Society: Interface* 9: 640–647.
- Aharoni H, Abraham Y, Elbaum E, Sharon E, Kupferman R. 2012. Emergence of spontaneous twist and curvature in non-euclidean rods: application to *Erodium* plant cells. *Physical Review Letters* 108: 238106.
- Aiton W. 1789. Hortus Kewensis, vol. 2 London, UK: Nicol.
- Albers F, Vander Walt JJA. 2007. Geraniaceae. In: Kubitzki K, ed. *The families and genera of vascular plants, vol. 9.* Berlin, Heidelberg, Germany and New York, NY, USA: Springer, 157–167.
- Aldasoro JJ, Navarro C, Vargas P, Saez L, Aedo C. 2002. California, a new genus of Geraniaceae endemic to the southwest of North America. Anales del Jardin Botánico de Madrid 59: 209–216.
- Barnett JR, Bonham VA. 2004. Cellulose microfibril angle in the cell wall of wood fibres. *Biological Reviews* 79: 461–472.
- Dawson C, Vincent JFV, Rocca AM. 1997. How pine cones open. *Nature* 390: 668.
- Elbaum R, Zaltzman L, Burgert I, Fratzl P. 2007. The role of wheat awns in the seed dispersal unit. *Science* 316: 884–886.
- Evangelista D, Hotton S, Dumais J. 2011. The mechanics of explosive dispersal and self-burial in the seeds of the filaree, *Erodium cicutarium* (Geraniaceae). *Journal of Experimental Biology* 214: 521–529.
- Fahn A, Werker E. 1972. Anatomical mechanisms of seed dispersal. In: Kozlowski TT, ed. Seed biology. New York, NY, USA: Academic Press, 152–221.
- Fiz O, Vargas P, Alarcón M, Aedo C, García JL, Aldasoro JJ. 2008. Phylogeny and historical biogeography of Geraniaceae in relation to climate changes and pollination ecology. *Systematic Botany* 33: 326–342.
- Fiz-Palacios O, Vargas P, Vila R, Papadopulos AST, Aldasoro JJ. 2010. The uneven phylogeny and biogeography of *Erodium* (Geraniaceae): radiations in the Mediterranean and recent recurrent intercontinental colonization. *Annals of Botany* 106: 871–884.
- Fratzl P, Elbaum R, Burgert I. 2008. Cellulose fibrils direct plant organ movements. Faraday Discussions 139: 275–282.
- Gillis PP, Mark RE. 1973. Analysis of shrinkage, swelling, and twisting of pulp fibers. *Cellulose Chemical Technology* 7: 209–234.
- Hammersley AP, Svensson SO, Hanfland M, Fitch AN, Hausermann D. 1996.
 Two-dimensional detector software: From real detector to idealised image or two-theta scan. *High Pressure Research* 14: 235–248.
- Herrera J. 1991. Herbivory, seed dispersal and the distribution of a ruderal plant living in a natural habitat. *Oikos* 62: 209–215.
- Jost L. 1907. Lecture XXXII: Movement resulting from swelling and contraction and from cohesion of imbibition water. In: Gibson RJH, ed. *Lectures on plant* physiology. Oxford, UK: Clarendon, 405–417.
- Lacey EP, Kaufman PB, Dayanandan P. 1983. The anatomical basis for hygroscopic movement in primary rays of *Daucus carota* ssp. *carota* (Apiaceae). *Botanical Gazette* 144: 371–375.
- Li Y, Beck R, Huang T, Choi MC, Divinagracia M. 2008. Scatterless hybrid metal-single-crystal slit for small-angle X-ray scattering and high-resolution X-ray diffraction. *Journal of Applied Crystallography* 41: 1134–1139.
- L'Heritier CL. 1792. *Geraniologia*. Paris, France and London, UK: Vienna & Strasbourg.
- Nadler M, Steiner A, Dvir T, Szekely O, Szekely P, Ginsburg A, Asor R, Resh R, Tamburu C, Peres M *et al.* 2011. Following the structural changes during zinc-induced crystallization of charged membranes using time-resolved solution X-ray scattering. *Soft Matter* 7: 1512–1523.

4698137, 2013, 2, Downloaded from https://nph.onlinelibrary.wiley.com/doi/10.1111/nph.12254 by Cochrane Israel, Wiley Online Library on [23/04/2025]. See the Terms conditions) on Wiley Online Library for rules of use; OA articles are governed by the applicable Creative Commons License

- Price RA, Palmer JD. 1993. Phylogenetic relationships of the Geraniaceae and Geraniales from rbcL sequence comparisons. *Annals of the Missouri Botanical Garden* 80: 661–671.
- Pufal G, Ryan KG, Garnock-Jones P. 2010. Hygrochastic capsule dehiscence in New Zealand alpine Veronica (Plantaginaceae). American Journal of Botany 97: 1413–1423.
- Reyssat E, Mahadevan L. 2009. Hygromorphs: from pine cones to biomimetic bilayers. *Journal of the Royal Society: Interface* 6: 951–957.
- Rüggeberg M, Speck T, Paris O, Lapierre C, Pollet B, Koch G, Burgert I. 2008. Stiffness gradients in vascular bundles of the palm *Washingtonia robusta*. Proceedings of the Royal Society B-Biological Sciences 275: 2221–2229.
- Stamp NE. 1984. Self-burial behaviour of Erodium cicutarium seeds. The Journal of Ecology 72: 611–620.
- Stamp NE. 1989a. Efficacy of explosive vs. hygroscopic seed dispersal by an annual grassland species. *American Journal of Botany* 76: 555–561.
- Stamp NE. 1989b. Seed dispersal of four sympatric grassland annual species of Erodium. Journal of Ecology 77: 1005–1020.
- Witztum A, Schulgasser K. 1995. The mechanics of seed expulsion in Acanthaceae. *Journal of Theoretical Biology* 176: 531–542.
- Yeo PF. 1984. Fruit-discharge-type in Geranium (Geraniaceae): its use in classification and its evolutionary implications. *Botanical Journal of the Linnean Society* 89: 1–36.
- Yeung EC. 1998. A beginner's guide to the study of plant structure. In: Karcher SJ, ed. *Tested studies for laboratory teaching, vol. 19.* Proc. 19th Workshop/ Conf. Assoc. Biology Laboratory Education (ABLE), 125–143.
- Young JAE, Kay RA, Burgess L. 1974. Dispersal and germination dynamics of broadleaf filaree, *Erodium botrys* (Cav.) Bertol. *Agronomy Journal* 67: 54–57.

Supporting Information

Additional supporting information may be found in the online version of this article.

- Fig. S1 Plots of average retardance values as a function of azimuthal angle, χ , displaying the change in the retardance around the cell wall.
- **Notes S1** The limit for detecting tilt angles based on polarized light microscopy
- **Movie \$1** Wet awn of *G. pusillum* bending as it dries. The clip is accelerated by a factor of 70.
- **Movie S2** Wet awn of *G. dolomiticum* coiling as it dries. The clip is accelerated by a factor of 140.

- **Movie \$3** Wet awn of *G. reflexum* coiling as it dries. The clip is accelerated by a factor of 140.
- **Movie S4** Wet awn of *P. peltatum* coiling as it dries. The clip is accelerated by a factor of 140.
- **Movie S5** Outer layer slightly coiling *E. gruinum* cells, probably representing the MidSL.
- **Movie S6** Outer layer coiling cells of *E. gruinum*, probably representing the OutSL. The clip is accelerated by a factor of 2. **Movie S7** Cells from the outer layer in *G. pusillum* twist as they dry.
- **Movie S8** Cells from the inner layer in *G. pusillum* twist as they dry.
- **Movie S9** Cells from the inner layer of *G. dolomiticum* coil as they dry. The clip is accelerated by a factor of 2.
- **Movie S10** Cells from the outer layer of *G. dolomiticum* coil as they dry.
- **Movie S11** Cells from the inner layer of *G. reflexum* twist as they dry.
- **Movie S12** Twisting cells from the outer layer of *G. reflexum*, probably representing the MidSL.
- **Movie S13** Coiling cells from the outer layer of *G. reflexum*, probably representing the OutSL.
- **Movie S14** The coiling inner layer of the *P. peltatum* awn. The clip is accelerated by a factor of 8.
- **Movie S15** Twisting cell groups isolated from the outer layer of the *P. peltatum* awn. The clip is accelerated by a factor of 4.
- Please note: Wiley-Blackwell are not responsible for the content or functionality of any supporting information supplied by the authors. Any queries (other than missing material) should be directed to the *New Phytologist* Central Office.